UNIVERSITY OF AMSTERDAM

UvA-DARE (Digital Academic Repository)

Understanding gene expression variability in its biological context using theoretical and experimental analyses of single cells

Kempe, H.

Publication date
2017

Document Version
Other version

License
Other

Link to publication

Citation for published version (APA):
Kempe, H. (2017). *Understanding gene expression variability in its biological context using theoretical and experimental analyses of single cells*. [Thesis, fully internal, Universiteit van Amsterdam].

General rights
It is not permitted to download or to forward/distribute the text or part of it without the consent of the author(s) and/or copyright holder(s), other than for strictly personal, individual use, unless the work is under an open content license (like Creative Commons).

Disclaimer/Complaints regulations
If you believe that digital publication of certain material infringes any of your rights or (privacy) interests, please let the Library know, stating your reasons. In case of a legitimate complaint, the Library will make the material inaccessible and/or remove it from the website. Please Ask the Library: https://uba.uva.nl/en/contact, or a letter to: Library of the University of Amsterdam, Secretariat, Singel 425, 1012 WP Amsterdam, The Netherlands. You will be contacted as soon as possible.

UvA-DARE is a service provided by the library of the University of Amsterdam (https://dare.uva.nl)

Download date:08 Nov 2025

Chapter 4

MeCP2 accelerates the transition rate of transcription repression dynamics measured at a defined chromatin locus in single cells

In collaboration with:
Diewertje Piebes, Ilona Vuist, G.J. van Belle,
Aadriaan B. Houtsmuller and Pernette J. Verschure
Adapted from: manuscript submitted for publication.

4.1 abstract

Gene expression is regulated by the complex interplay of transcription factors and cofactors that directly or indirectly bind to DNA and alter chromatin composition. Here, we used time-lapse microscopy to analyze the repression kinetics when modulating chromatin state, employing a reporter gene array. The array consists of lac and tet operator binding sequences allowing targeting of fluorescent lac and tet repressors tagged with chromatin regulatory proteins of interest to control the expression of a CFP reporter gene, also encoding additional 3' UTR MS2 hairpins to allow quantification of newly synthesized transcripts in real-time. After inducing transcription repression by removing the targeted transcriptional activator, we observe that transcription initiation of the reporter gene transiently continues whereas the transcriptional activator is instantly lost from the array. Our data show a biphasic transcription repression response representing the actual decrease in transcripts at the reporter gene array and a preceding response time. We observe that targeting of the epigenetic reader protein methyl-CpG-binding protein 2 (MeCP2) significantly accelerates the transition rate of transcription repression, while the rate at which transcripts diffuse from the array is unaffected. We conclude that MeCP2 is able to facilitate the response to signals suppressing active transcription

4.2 Introduction

Epigenetic chromatin composition provides a dynamic means of creating chromatin with distinct features and properties that regulate chromatin-associated processes. Transcriptional activity [122, 123] can be altered via binding of chromatin-associated proteins and local changes in chromatin structure [124, 125, 125, 126]. Transcription is not only regulated by recruitment of RNA polymerase II at promoters, but also by proteins regulating the ability of RNA polymerase II to penetrate chromatin barriers and facilitate its processivity [81, 127–131]. Transcription regulatory elements, such as the transcription start site, promoter/enhancer regions, and body of the gene exhibit defined histone modification patterns that are involved in regulating gene activation or repression [132]. Methyl-CpG-binding protein 2 (MeCP2) is an epigenetic regulatory protein best described as a facilitator of setting gene expression programs [133] acting as a key chromatin structure regulator [133–136] and transcriptional regulator recruiting corepressors [137–139] (or activators [140, 141]). MeCP2 can alter chromatin folding as it binds chromatin-remodeling proteins such as Brahma and ATRX [142, 143]. Moreover, MeCP2 can bind methylated DNA and recruit repressive proteins such as mSin3a and histone deacetylases (HDACs) [139, 144, 144–147]. In addition, the N-terminal domain of MeCP2 has been shown to bind Heterochromatin Protein 1 (HP1) [148] , which is typically associated with the formation of transcriptionally silent chromatin as it binds through its chromodomain to tri-methylated histone H3 lysine 9 (H3K9me3) and recruits histone methyltransferase enzymes [149] . We recently showed that targeted binding of MeCP2 elicits chromatin unfolding and triggers the loss

of HP1γ without any apparent change in expression of the genomically integrated reporter gene [150] . In contrast, evidence has been provided that MeCP2 binds to promoters of active genes and induces gene activity via cAMP response element-binding protein (CREB) [151]. Overall the connection between epigenetic chromatin composition and the precise role of regulatory proteins in transcription regulation and whether this is achieved via altering chromatin composition is unclear. In this study, we took a single cell approach to investigate the dynamics of induced repression on a transcriptionally active reporter gene array. We used the U2OS 2-6-3 clone containing a multicopy integrated reporter gene cassette (Figure 4.1A-D) [152] , which consists of lac and tet operator (lacO and tetO) binding sequences, a CFP-SKL reporter gene, and a gene encoding MS2 hairpin loops. Binding of fluorescently tagged lac repressor (lacR) and tet repressor (tetR) to lacO and tetO binding sequences allows visualization as well as modulation of the reporter gene array while the MS2 hairpin repeats enable visualization of newly synthesized transcripts by binding of YFP-tagged MS2 protein. MS2 tagging at reporter gene arrays has previously been explored extensively to study transcriptional activation [35, 152–163] . However the dynamic behavior of transcripts and other involved factors when switching from a transcriptionally active to an inactive state has only recently started to be addressed [164]. We measured induced repression of an activated reporter gene in absence and presence of the epigenetic modulator MeCP2. Briefly, we show that the decrease in the number of transcripts produced at the reporter gene array upon induction of repression significantly lags behind the rapid release of transcriptional activators. These findings suggest that new transcription initiation events transiently persist, in spite of the absence of the targeted transcriptional activator at the reporter gene array. Interestingly, when MeCP2 is targeted to the reporter gene array the transition rate is significantly shorter (while the transcript decrease kinetics are similar to those observed in non-targeted cells), suggesting that the role of MeCP2 when being associated with actively transcribed chromatin is to help keep actively transcribed chromatin in such a state that the response to signals suppressing transcription is accelerated.

4.3 Results

4.3.1 Experimental approach

We used time-lapse microscopy to analyze the dynamics of transcription repression when modulating chromatin state, employing a reporter gene array. We used the U2OS 2-6-3 cell line containing a multicopy integrated reporter gene cassette [152] , consisting of 200 copies of a construct containing repeats of lacO (256x) and tetO (96x) sequences which allows for the visualization of the array by targeting fluorescently tagged versions of lacR and tetR to binding sequences of the cassette (Figure 4.1A-D). In addition, lacR or tetR can be used to target additional fused transcription or chromatin modifying factors to the array to study their effect on transcription of a CFP-tagged SKL reporter gene extended with DNA encoding for MS2 RNA

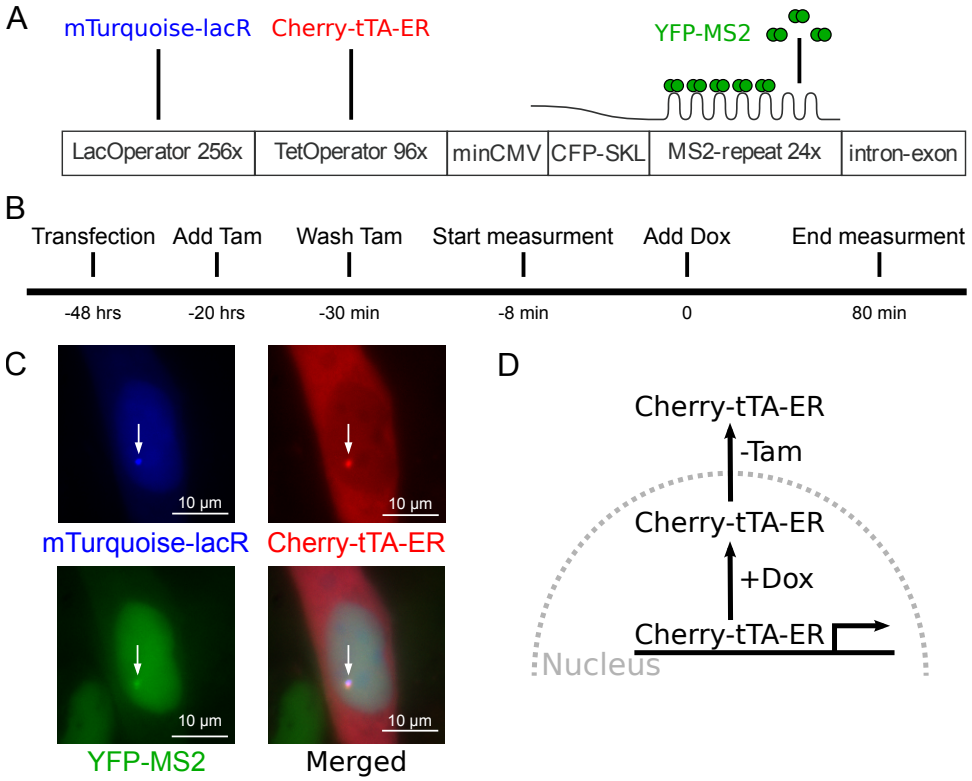

FIGURE 4.1: **Experimental approach.** A) Schematic representation of the reporter gene cassette. LacO is used for mTurquoise tagged lacR targeting and localization at the array. TetO Cherry-tTA-ER transcriptional activator binding is used to induce transcription of the CFP-SKL reporter gene consisting of a minimal CMV promoter, an SKL peroxisomal localization signal, and MS2 hairpin loops. YFP-MS2 coat protein binding to the MS2 repeat enables time-lapse microscopy transcription measurements at the reporter gene array. The intron-exon sequence attracts mRNA processing complexes. B) Schematic representation of the experimental time line. Cells are transfected at -48 hours. The addition of Tamoxifen (20 hours) allows Cherry-tTA-ER to enter the nucleus and bind the tetO array in the absence of doxycycline thereby activating reporter gene activity. The medium is replaced by microscopy medium (-30 min) thereby removing Tamoxifen. The microscopy imaging is started at -8 min and addition of doxycycline is at t=0. Cells are imaged for 90 minutes. C) The images show a typical representation of a cell expressing mTurquoise-lacR (blue), Cherry-tTA-ER (red) and YFP-MS2 (green). The arrow points to visualization of the reporter gene array by mTurquoise-lacR, Cherry-tTA-ER and YFP-MS2 levels immediately after doxycycline (Dox) induction (t=0). The image is a z-projection of a fluorescence microscopy stack, and the bar represents 10 μm. D) Schematic representation of the treatments to release transcriptional activator (Cherry-tTA-ER) from the reporter gene array to measure transcription repression kinetics. Tamoxifen (Tam) regulates the localization of Cherry-tTA-ER in the nucleus while doxycycline interferes with tetO binding at the reporter gene array.

hairpin loops (Figure 4.1A-D). MS2 hairpins at the transcribed genes can in turn be used to quantify transcriptional activity of the system by measuring intensities of fluorescently tagged MS2 protein. To activate the reporter gene we used tetR tagged with the C-terminal domain of the tetracycline controlled transactivator VP16 (tTA), which increases and reduces gene activity in absence and presence of tetracycline (or its derivate doxycycline), respectively. To be able to regulate nuclear translocation, tTA was also fused to a Cherry tagged version of the estrogen receptor ligand binding domain (Cherry-tTA-ER). mTurquoise tagged lacR was used to visualize and track the reporter gene array. In a typical experimental set-up, the U2OS 2-6-3 cells were treated overnight with Tamoxifen which binds to the ER ligand binding domain and

thereby induces nuclear translocation of Cherry-tTA-ER. Cells were then imaged by confocal microscopy after removing Tamoxifen to stop Cherry-tTA-ER transport into the nucleus, and prior and after adding doxycycline to rapidly release it from the reporter gene array (Figure 4.1B and D). To study the effect of altering chromatin structure of the reporter gene array on transcriptional regulation, we targeted CFP-lacR fused to MeCP2 [136, 140, 150, 165] to the lacO binding sequences within the reporter gene array.

	-Tam	+Tam
-Dox	76.5 min	160.3 min
+Dox	2.1 min	21.3 min

TABLE 4.1: **The half-life ($t_{\frac{1}{2}}$) decrease in Cherry-tTA-ER at the reporter gene array in minutes.** A rapid decrease in Cherry-tTA-ER localization at the reporter gene array is achieved by the presence of doxycycline and absence of Tamoxifen. This setup disables transport of Cherry-tTA-ER to the nucleus and inhibits its binding to the gene array.

4.3.2 Biphasic transcription repression

We measured the decrease in transcriptional activator (Cherry-tTA-ER) and transcripts (YFP-MS2) at the array in real-time when inducing the removal of Cherry-tTA-ER from the array (-Tam/+Dox). As controls we measured the Cherry-tTA-ER, YFP-MS2 and mTurquoise-lacR levels at the reporter gene array in response to the presence and/or absence of Tamoxifen and doxycyline, i.e. +Tam/+Dox, -Tam/-Dox, +Tam/-Dox (Figure 4.4). Both Cherry-tTA-ER and YFP-MS2 data fitted well to an exponential decline function (Figure 4.5 and 4.6). We observed that the abundance of Cherry-tTA-ER and YFP-MS2 at the reporter gene array decreased with a median half-life ($t_{\frac{1}{2}}$) of 2 minutes and 8 minutes, respectively (Figure 4.2A, B, C, D). As an additional control, we measured whether the decrease in Cherry-tTA-ER at the reporter gene array induces a decrease in the level of histone acetyl transferase (HAT) GCN5 at the array. GCN5 is a bromodomain containing HAT known to accompany VP16 at the multicopy array in U2OS 2-6-3 cells and to anchor chromatin-modifying complexes to promoter nucleosomes [150, 166, 167]. We observed that the decrease in GCN5 at the reporter gene array (median $t_{\frac{1}{2}}$ is 3.4 minutes) is no different from the decrease in Cherry-tTA-ER (Figure 4.2E), indicating that transcription activator removal-induced gene repression accompanies a drop in transcription regulatory proteins such as HAT enzymes.

To fit the exponential decline of YFP-MS2 transcripts we included the possibility that this decline consists of a lag time between the release of Cherry-tTA-ER and the actual decrease in MS2-tagged transcripts (Figure 4.2F). We noted that the decrease in YFP-MS2 is preceded by a transition phase with a median time of 5 minutes (Figure 4.2F). Depending on the residence time of RNA polymerase II at the reporter gene we can infer whether transcription continues after removal of the transcriptional activator from the array. Darzacq et al. estimated that the mean residence time of RNA polymerase II is 517 seconds at this multicopy reporter gene

array[155]. The sum of the reported residence time of RNA polymerase II and the time at which transcriptional activator Cherry-tTA-ER is removed from the reporter gene array (dashed gray lines in Figure 4.5 and 4.6) provides a rough estimation for the expected time of complete YFP-MS2 transcript loss. We refer to this time as the fraction of enduring transcription. At this time point at which all transcripts are expected to be lost from the array, on average 23% of the initial number of YFP-MS2 transcripts are still present at the reporter gene array (Figure 4.2G). To determine if slow diffusion leads to underestimating the observed YFP-MS2 transcript levels, we applied fluorescence recovery after photobleaching (FRAP). Briefly, we bleached an area with a diameter spanning the reporter gene array and determined the recovery of fluorescence at 1 second time intervals. The observed diffusion coefficients at the array for YFP-MS2 are 0.3 $\mu m^2 s^{-1}$ and 0.03 $\mu m^2 s^{-1}$ (Figure 4.9A, B, Table 4.1). These FRAP data indicate that the experimentally measured decrease in YFP-MS2 transcripts at the reporter gene array, upon removing Cherry-tTA-ER from the array (minute-scale), is much slower than the estimated second-scale YFP-MS2 transcript diffusion rate.

4.3.3 MeCP2 facilitates increased transcription repression responsiveness

To investigate the contribution of local chromatin structure on transcription repression dynamics, we measured the response of the system upon targeting MeCP2 to the reporter gene array. We observed that the abundance of Cherry-tTA-ER at the MeCP2 targeted gene array decreased with a median half-life of 1.5 minutes, slightly faster than the half-life of Cherry-tTA-ER in control cells (Figure 4.2A, C). Similarly, we noted that the decrease of YFP-MS2 at the MeCP2 targeted reporter gene array had a comparable median half-life to that observed in control cells (median $t_{\frac{1}{2}}$ is 6.8 minutes, Figure 4.2B, D). Also the percentage of YFP-MS2 transcripts at the MeCP2 targeted reporter gene array at the time point that Cherry-tTA-ER is expected to be lost from the array is similar to the percentage in control cells, 19% versus 23%, respectively (Figure 4.2G). Notably, when MeCP2 is present at the reporter gene array, we observed a significantly shorter transition time preceding the decrease in transcripts compared to the transition rate in control cells (median transition rate in MeCP2 targeted cells is 2 minutes versus 5 minutes in control cells) (Figure 4.2F). These data suggest that at the MeCP2 targeted array, accelerated repression is achieved via a change in the transition rate instead of the actual decrease in transcripts.

To explore whether MeCP2 targeting has an effect on the size, mobility and transcriptional state of the array, we tracked the motion of the MeCP2 targeted array and measured its size and levels of Cherry-tTA-ER and YFP-MS2 (Figure 4.7, 4.8). On average we observed an increased nuclear motion (Figure 4.7) but unaltered size of the array upon MeCP2 targeting (Figure 4.8C), whereas we did not observe a significant difference in levels of Cherry-tTA-ER and YFP-MS2 at the array either in the presence or absence of MeCP2 (Figure 4.8A-C). To further illustrate the correlation between Cherry-tTA-ER and YFP-MS2 levels, we plot the correlation between

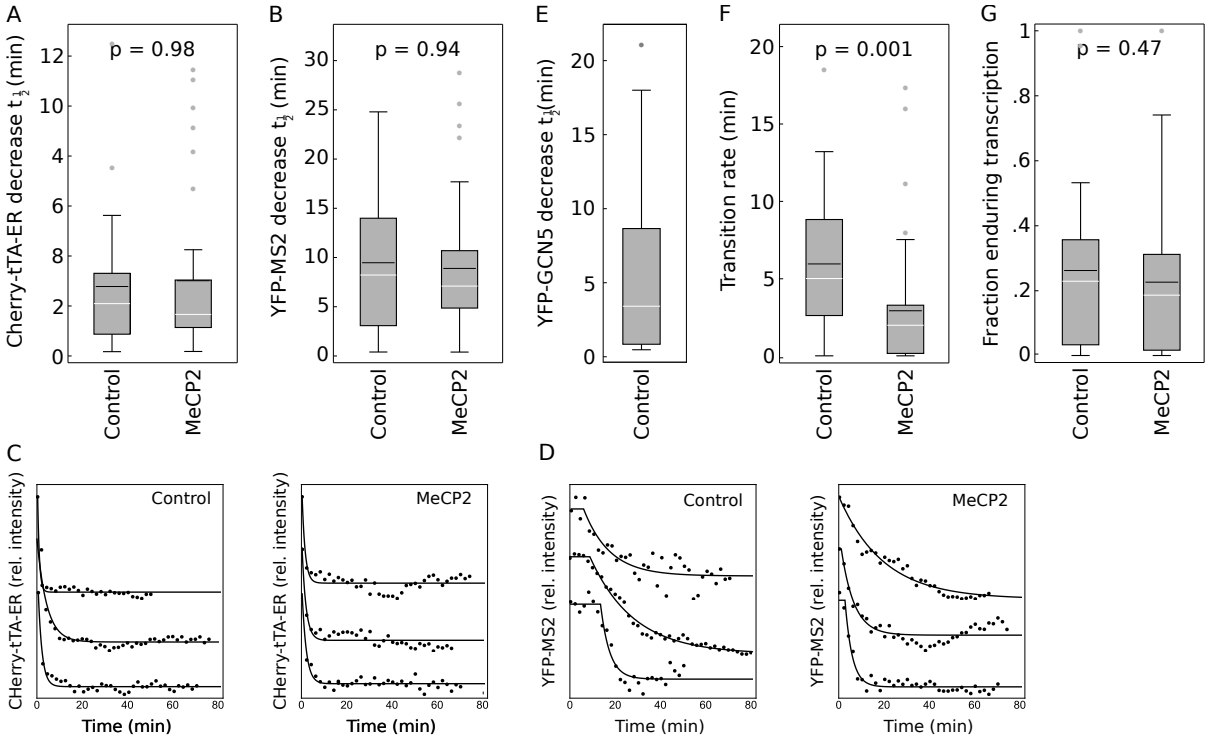

FIGURE 4.2: **Transcription repression dynamics at the reporter gene array.** Measurements at the reporter gene array in control and MeCP2 targeted U2OS 2-6-3 cells after doxycycline-induced release of Cherry-tTA-ER. The p-values shown are obtained by non-parametric Mann-Whitney U testing. A) The half-life ($t_{\frac{1}{2}}$) for the decrease in transcriptional activator Cherry-tTA-ER localization at the reporter gene array. B) The $t_{\frac{1}{2}}$ decrease in YFP-MS2 transcripts produced from the reporter gene array. C) Representative single cell traces showing the decrease in Cherry-tTA-ER in control and MeCP2 targeted cells. D) Representative single cell traces showing the decrease in YFP-MS2 in control and MeCP2 targeted cells at the reporter gene array. E) The $t_{\frac{1}{2}}$ decrease of acetyltransferase GCN5 at the reporter gene array. F) The transition rate of transcription repression dynamics at the reporter gene array. G) The fraction of enduring transcription at the reporter gene array. We interpret this fraction as the sum of the reported residence time of RNA polymerase II and the time at which transcriptional activator Cherry-tTA-ER is removed from the reporter gene array.

Cherry-tTA-ER levels in the nucleus and at the array as well as between Cherry-tTA-ER and YFP-MS2 levels both at the array. We observed a positive correlation between Cherry-tTA-ER nuclear and array bound levels in both control and MeCP2 targeted cells ($\rho = 0.72$ and 0.61, respectively), which indicates that in our experimental set-up Cherry-tTA-ER binding at the reporter gene array is not saturated. (Figure 4.8D). Plotting the correlation between Cherry-tTA-ER and YFP-MS2 levels at the reporter gene array in control and MeCP2 targeted cells ($\rho = -0.32$ and -0.13, respectively) shows in both cases a negative correlation. This suggests that the transcriptional response is saturated already at initial transcriptional activator levels before Cherry-tTA-ER is lost from the array, indicating that minor fluctuations in Cherry-tTA-ER do not affect the YFP-MS2 output. (Figure 4.8E).

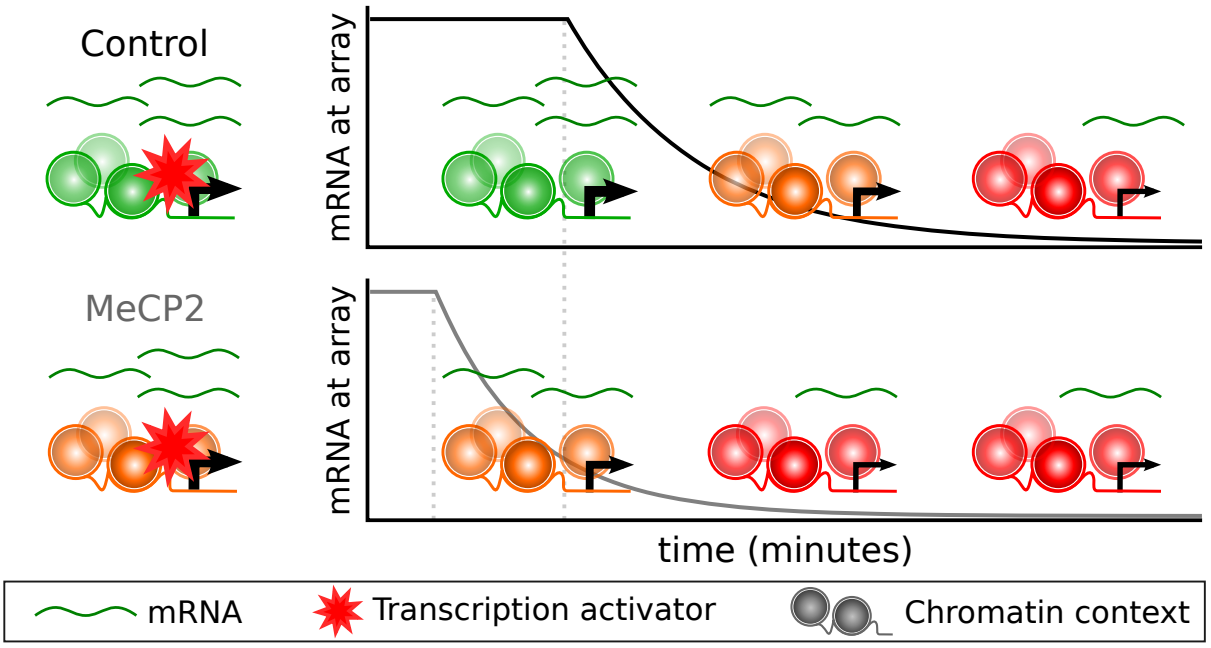

FIGURE 4.3: **Single cell transcription repression indicates a chromatin-dependent transition rate.** The cartoon illustrates the main characteristics of the measured repression dynamics, illustrating the decrease in transcripts (green lines) in real-time upon releasing a transcriptional activator (red star). Control cells (represented by the black line) display a prolonged transition time (dashed gray lines) compared to the repression in MeCP2 targeted cells (represented by the gray line). We propose that local chromatin context (represented by the colored DNA-nucleosome-promoter cartoon) sets the transition rate of transcription repression by temporally allowing new transcription initiation events.

4.4 Discussion

The U2OS 2-6-3 reporter gene array provides an effective tool to measure gene activity in a local chromatin context since it allows local transcription modulation without affecting global transcriptional outputs. We show biphasic transcription repression, i.e. a transition phase until transcripts are lost from the array after which transcript levels decrease exponentially. Targeting of MeCP2 to the reporter gene array accelerates the transition rate while the kinetics of the decrease in transcripts at the array are unaffected.

Our data point out that the observed transition rate in transcription repression compared to fast loss of transcriptional activator from the array cannot be explained by slow diffusion of YFP-MS2 transcripts that are produced by the reporter gene since the second-scale YFP-MS2 diffusion hardly contributes to the minute-scale measured decrease in YFP-MS2 transcripts. Our data suggest that endogenous transcriptional activators are still able to initiate transcription and that engaged RNA polymerase II continues producing mRNA and creating new binding sites for YFP-MS2 protein even beyond the point when the initial transcriptional activator is lost. We show that MeCP2 facilitates the transition time of single cells to become transcriptionally repressed. Our data show that the transcriptional activator levels at the array in MeCP2

targeted and control cells are very similar (Figure 4.8A). Moreover, we noted that the activated reporter gene array both in control and MeCP2 targeted cells is rather insensitive to a decrease in transcriptional activator (Figure 4.8E and Figure 4.6, 4.7). We conclude that once a gene is active, the period of activity is mainly determined by chromatin structural alterations thereby introducing a transition rate in transcription repression.

For instance histone exchange processes including incorporation of variant and/or canonical histones, and their posttranslational modifications, are efficient mechanisms to lengthen the response time in altering gene activity [168] In principle, it is known that passage of RNA polymerase II over coding regions of genes is accompanied by a disruption of nucleosome structure. Depending on the level of gene transcription (low, moderate or high) chromatin structural alterations occur more frequently, but in all cases transcription shutdown is accompanied by re-formation of a more spaced nucleosomal state and histone exchange suppression [168, 169]. We propose that local chromatin context determines whether new transcription initiation events take place, or whether the chromatin first needs to change its structure thereby regulating transcription repression at the level of time delayed responsiveness (Figure 4.3). In this context, Bintu et al. illustrated the dynamic behavior in gene activity upon recruiting epigenetic regulatory proteins associated with a broad range of chromatin modifications [164] . The authors identified that different regulators evoke diverse modes of action via an altered initial transition rate and time scale of operation.

Since the studied reporter gene array is a multicopy array, we expected that MS2-tagged transcript measurements in single cells would represent an average transcript number of all single reporter genes within the array and that it would provide low cell-cell variability in reporter gene activity. However, we observe substantial variability in transcriptional activity and response time between single cell samples (Figure 4.5, 4.6, and 4.2E). This variation might be caused by variation in Cherry-tTA-ER expression levels, heterogeneity in the cell-cycle status, or a combination of factors. Since transcription initiation events are known to correlate within the same locus [29, 170] all genes within the reporter gene array might cycle simultaneously between 'on' and 'off' states. In this context, it should be noted that the locus of the reporter gene array spans 200 times 3.3 kb.

Determining the molecular aspects of transcription dynamics is still a central challenge to understanding eukaryotic gene expression regulation. Large protein complexes assemble and disassemble at genes within seconds [171], nucleosome exchange occurs in the order of minutes to hours depending on the genomic location [172] and transcript production is shown to follow complex bursting dynamics. Transcriptional kinetics of endogenous genes is characterized in single cells measuring transcription cycling of a short-lived luciferase reporter gene inserted into the mammalian genome [28, 56, 173]. By inferring dynamic on/off state kinetic parameters from a mathematical approach, Suter et al. showed that for each gene, specific endogenous regulatory sequences determine its set of kinetic transcription parameters. Many studies used

a random telegraph model to describe transcriptional kinetics, stating that a gene can be in a transcriptionally active or inactive state [174]. Rybakova et al. and Schwabe et al. described transcription cycling according to a ratchet model, showing transitioning between 'on' to 'off' and 'off' to 'on' states via a multistep process[175, 176]. The progression through the ratchet in this model is locked by irreversible covalent reactions, representing for instance chromatin structural changes induced by posttranslational histone modifications. During the transition from the 'on' to 'off' state, transcription is still able to proceed. Therefore, a ratchet-like model predicts a delayed deactivation of transcription. Up until now experimental work has failed to show triggered transcriptional deactivation, hence the delay in response to transcriptional deactivation. In our experimental set-up, the U2OS 2-6-3 reporter gene array enabled us to experimentally measure triggered transcription repression in single cells of an activated reporter gene using time-lapse microscopy. Upon targeting MeCP2 to the reporter gene array, we observe a diminished transition rate in transcription repression, indicating a more rapid transitioning from the 'on' to 'off' phase. Of interest, the transcriptional activation levels seem to be increased by targeting MeCP2 to the array. Since MeCP2 effectively decreased the 'on' phase, such an effect can only be obtained by faster transitioning through the 'off' phase. This would imply a double role for MeCP2 in transcription and might add to the much-discussed role of MeCP2 in gene expression.

4.5 Materials and Methods

Cell Culture

U2OS 2-6-3 YFP-MS2 expressing cells [152] were cultured in DMEM, glutamax (Gibco, Thermo Fisher Scientific Inc.) 10% tet approved FCS (Clontech Laboratories, Inc., Takara biocompany), 1% PS (Gibco, Thermo Fisher Scientific Inc.) and $40\mu g/ml$ G418 (Gibco, Thermo Fisher Scientific Inc.) at 37°C under 10% CO2. Cells were transfected using lipofectamin 2000 according to manufacturers instruction. Tamoxifen (Sigma) was added at 1mM concentration 20 hours prior to the experiment unless stated otherwise. Doxycyclin was added to a final concentration of 1 $\mu g/ml$. The medium was replaced with Microscopy Medium, (137mM NaCl, 20mM D-glucose, 20mM Hepes, 5.4 mM KCl, 1.8 mM CaCl2, 08 mM MgSO4) 30 min before imaging.

4.5.1 Plasmids

Cherry-tTA-ER was a gift from SM Janicki and mTurquoise tagged lacR from MS Luijsterburg. CFP-lacR-MeCP2 was assembled with a Gibson assembly[177] using EGFP-lacR-MeCP2 [150] and the CFPs3a (Clontech laboratories, Inc., Takara biocompany) vector using the following

primers CCGGACTCAGATCTCGAGCATCCATGGTGAAATATGTAAC , GGGCGATCGTC-TAGAGTCGAGTTTAGTGAACCGTCAGATC and the reverse complement sequence of both primers.

4.5.2 Time-lapse microscopy measurements

For time-lapse microscopy , U2OS 2-6-3 cells stably expressing YFP-MS2 were transfected with mTurqoise tagged lacR and tTA-Cherry-VP16 in Mattek dishes. 1mM Tam was added 20 h before the experiment to enable Cherry-tTA-ER diffusion into the nucleus allowing Cherry-tTA-ER binding at the tetO binding sites of the integrated reporter gene array. Prior to the single cell real-time microscopy measurements, Tam was washed away from the medium disabling Cherry-tTA-ER to diffuse into the nucleus thereby lowering its concentration in the nucleus. After 30 minutes the cells are adjusted in the microscopy chamber and at t=0 Dox was added to an end concentration of $1\mu g/ml$, inducing a fast release of Cherry-tTA-ER from the tetO binding sites. The amount of Cherry-tTA-ER at the reporter gene array is measured using real-time wide-field microscopy imaging for up to 90 minutes. The time-line of treatments is shown in Figure 4.1C. The accumulation of Cherry-tTA-ER and YFP-MS2 at the mTurqoise-lacR labeled reporter gene array can be measured by means of mCherry, mTurqoise, and YFP measurements using a wide field microscope. We used a Zeiss Axiovert 200m (Zeiss, Germany) with a Cairn xenon arc lamp (Cairn Research, UK) with monochromator (0.30nm) and Zeiss 100x 1,4NA oil objective. The microscope is equipped with an incubator and an objective heater and heated to 37°C. Every 2 minutes images were taken with a cooled CCD camera (Coolsnap HQ, USA) using the following filters: CFP/mTurqouise: BP 470-30 YFP: BP 535-30 RFP: BP 620-60. Although we used both CFPs3a as well as mTurquoise, the same settings were used to ensure the same photography set-up for later comparison of time series.

4.5.3 Image analysis

In the first image of each time series, all acquired channels (YFP, RFP and CFP channels to monitor mRNA-YFP-MS2, Cherry-tTA-ER and mTurquoise-lacR, respectively) were averaged to identify the center coordinates of the reporter gene array. These coordinates were used in the "SpotTracker2D" [178] extension in ImageJ to track the reporter gene array at all time points. The obtained center coordinates of the reporter gene array were used to measure YFP, Cherry and mTurqoise or CFP intensities averaging over an area of 5 by 5 pixels ($= 0.934\mu m \times 0.934\mu m$) centered at these coordinates. At each time point we corrected for background intensity by subtracting the average of an equally sized background spot from within the nucleus. When the default background spot did not fall within the nucleus, we manually selected another one. Each single-cell time series was normalized to the maximum and minimum intensity spot of the image series.

4.5.4 Fluorescence Recovery After Photobleaching (FRAP)

We used a Leica SP5 confocal laser-scanning microscope equipped with a 40x/1.2NA HCX PL APO CS oil-immersion objective (Leica), an argon laser and an AOTF. For FRAP analysis a cell was scanned at 514 nm excitation with short intervals (585 ms) at low laser power (zoom 8 with 68.9 nm pixelsize). After 10 scans a high intensity (100% laser power) 650 ms bleach pulse at 488 nm was applied to a photobleaching spot with a diameter of 2.5 mm spanning the reporter gene array. Subsequently, the recovery of the fluorescence intensity in the photobleached spot was followed for another 20 seconds at 1s intervals and 300 seconds at 3s intervals. All curves were normalized to baseline fluorescent intensity post-bleach and averaged. The Lecia LASAF software was used for image acquisition and data extraction. We analyzed the FRAP data by fitting bi-exponentially the mRNA bound fraction and the non-bound freely diffusing YFP-MS2 fraction.

$$I(t) = 1 + A_1 e^{-\lambda_1 t} + A_2 e^{-\lambda_2 t} \tag{4.1}$$

We constrained both fits to use the same recovery rates ($\lambda 1$ and $\lambda 2$) since both fits consider the same mRNA-YFP-MS2 and YFP-MS2 molecules.

4.5.5 MS2 diffusion model

From the FRAP data we calculated the diffusion coefficient using:

$$D = 0.224 \frac{\omega}{t_{\frac{1}{2}}} \tag{4.2}$$

[179], in which D is the diffusion coefficient in $\mu m/s$, ω is the diameter of the bleached spot of the FRAP experiment. We constructed a two-dimensional finite difference diffusion model that provides diffusion in space and time (Figure 4.9 and Table 4.2). The model calculates the concentration at a certain time point and position based on the concentrations at this position and its direct surroundings at the previous time point. We generated a circular shaped grid with a diameter of 15 μm and we used a grid size of 0.1 μm. The transcription site is considered to have the same size as the average reporter gene array size within our experiments (2.45 μm^2, data not shown) and the reporter gene array is considered to be located at the center of the nucleus. We did not consider degradation or transport to the cytoplasm in the model. From the FRAP data we extracted the ratio between mRNA-MS2-YFP and MS2-YFP in the nucleus (0.25:0.75) and the transcription spot (0.73:0.27). From the FRAP data we can also calculate the average intensity ratio between the nucleus and the transcription spot. (0.27:0.73). Scaling the ratios obtained from the bi-exponential fit with the spot intensity ratio shows that there is

as much of YFP-MS2 present in the nucleus as at the transcription spot. However, mRNA-MS2-YFP is almost 8 times more abundant at the transcription spot. These ratios are summarized in Table 4.2 and used as starting conditions of the diffusion model.

Molecule	Location	Relative amount (a.u.)
MS2-YFP	Nucleus	0.206
mRNA-MS2-YFP	Nucleus	0.067
MS2-YFP	Reporter array	0.193
mRNA-MS2-YFP	Reporter array	0.533

TABLE 4.2: **Relative amount of MS2 fractions in the nucleus and at the reporter gene array.** The data show the calculated start condition measurements used for the diffusion model. MS2-YFP fractions are based on pre-bleach intensities of FRAP data and fractions (A1 and A2) from the fitted bi-exponential functions.

Acknowledgements

PJV acknowledge systems biology funding from the Science Faculty of the University of Amsterdam. We acknowledge funding from The Netherlands Dutch Research NWO-Meervoud 837.000.001 to PJV. We thank the van Leeuwenhoek Centre for Advanced Microscopy, SILS/UVA for the use of their microscope facility and expertiseThe members of the SSB/NOG group for critical discussions.

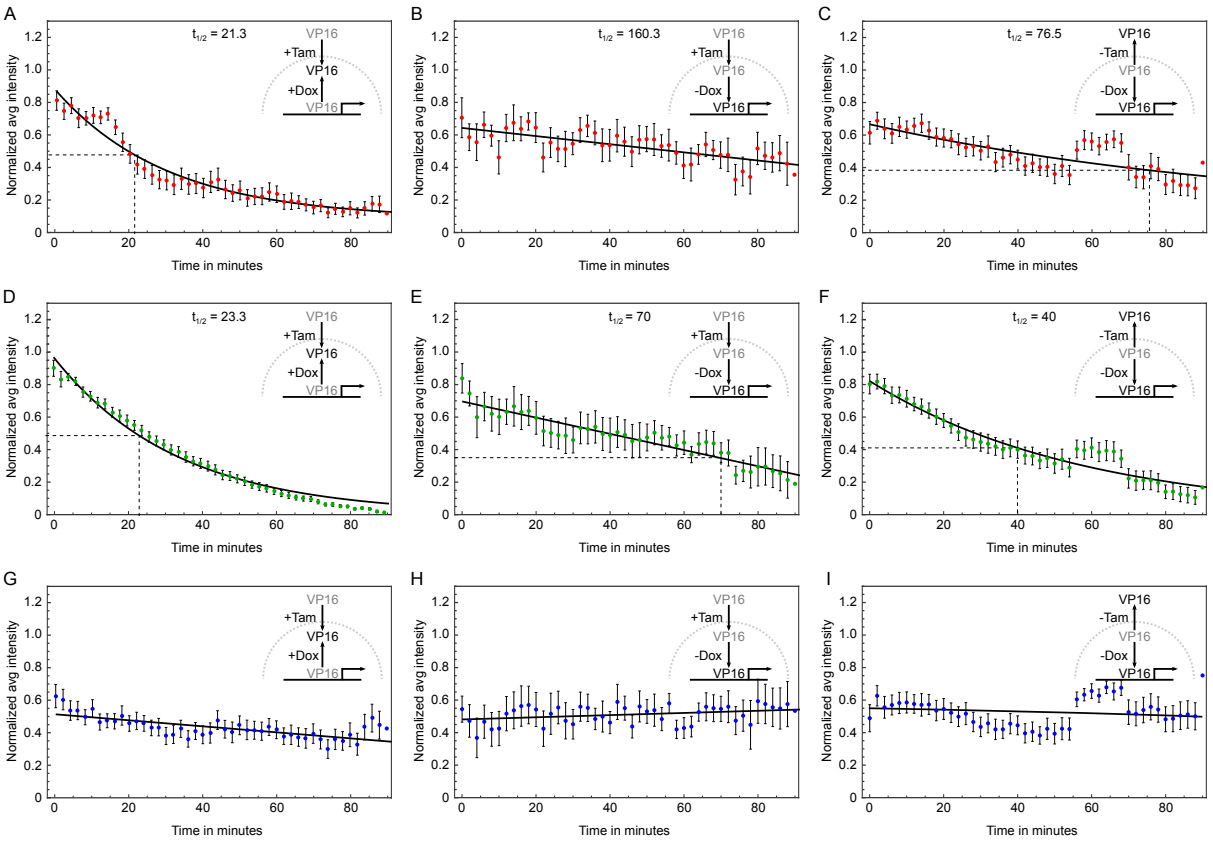

FIGURE 4.4: **Cherry-tTA-ER, YFP-MS2 and mTurquoise-lacR time-lapse microscopy measurements in the presence and/or absence of doxycycline and Tamoxifen.** A), (D), (G) The decrease in Cherry-tTA-ER transcriptional activator (A), MS2-YFP transcripts (D), and mTurqoise-lacR (G) from the reporter gene array in U2OS 2-6-3 cells in the presence of both Tamoxifen and doxycycline (+Tam/+Dox). (B), (E), (H) The decrease in Cherry-tTA-ER transcriptional activator (B), MS2-YFP transcripts (E), and mTurqoise-lacR (H) at the reporter gene array in U2OS 2-6-3 cells in the presence of Tamoxifen and absence of doxycycline (+Tam/-Dox). (C), (F), (I) The decrease in Cherry-tTA-ER transcriptional activator (D), MS2-YFP transcripts (F), and mTurqoise-lacR (I) at the reporter gene array in U2OS 2-6-3 cells in the absence of both Tamoxifen and doxycycline (-Tam/-Dox). The cartoon insert represents the experimental set-up of different subfigures. The dots show the mean normalized intensity at each time point. The error bar shows the standard error of the mean. The half-life (t1/2) of the decrease in Cherry-tTA-ER transcriptional activator and MS2-YFP transcripts at the reporter gene array is shown at the top-center of each plot and is indicated by the dashed lines.

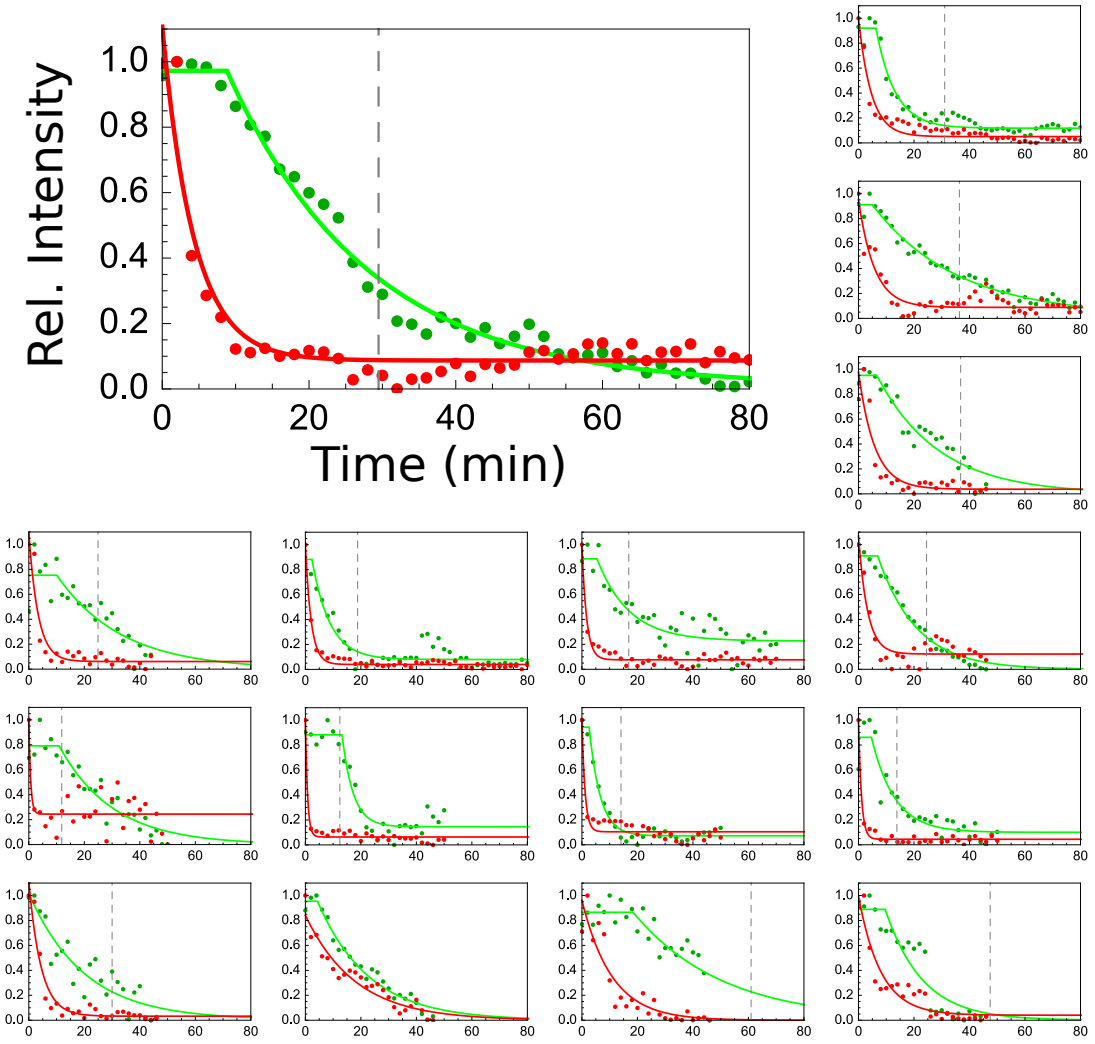

FIGURE 4.5: **Single cell measurements of the decrease in Cherry-tTA-ER transcriptional activator and YFP-MS2 transcripts in U2OS 2-6-3 control cells.** The plots show the decrease in YFP-MS2 transcripts (green) and Cherry-tTA-ER transcriptional activator (red) at the reporter gene array in U2OS 2-6-3 cells upon removing Cherry-tTA-ER from its tetO binding sequences in the presence of doxycycline and absence of Tamoxifen. The data is fitted to an exponential function with or without a delay for YFP-MS2 and Cherry-tTA-ER dynamics, respectively. The dashed line gives the time point at which Cherry-tTA-ER is depleted from the reporter gene array with an additionally added 517 seconds representing the average RNA polymerase II residence time at the reporter gene. The fitted curves that deviated on average more than 10% from each data point were not used for further analyses.

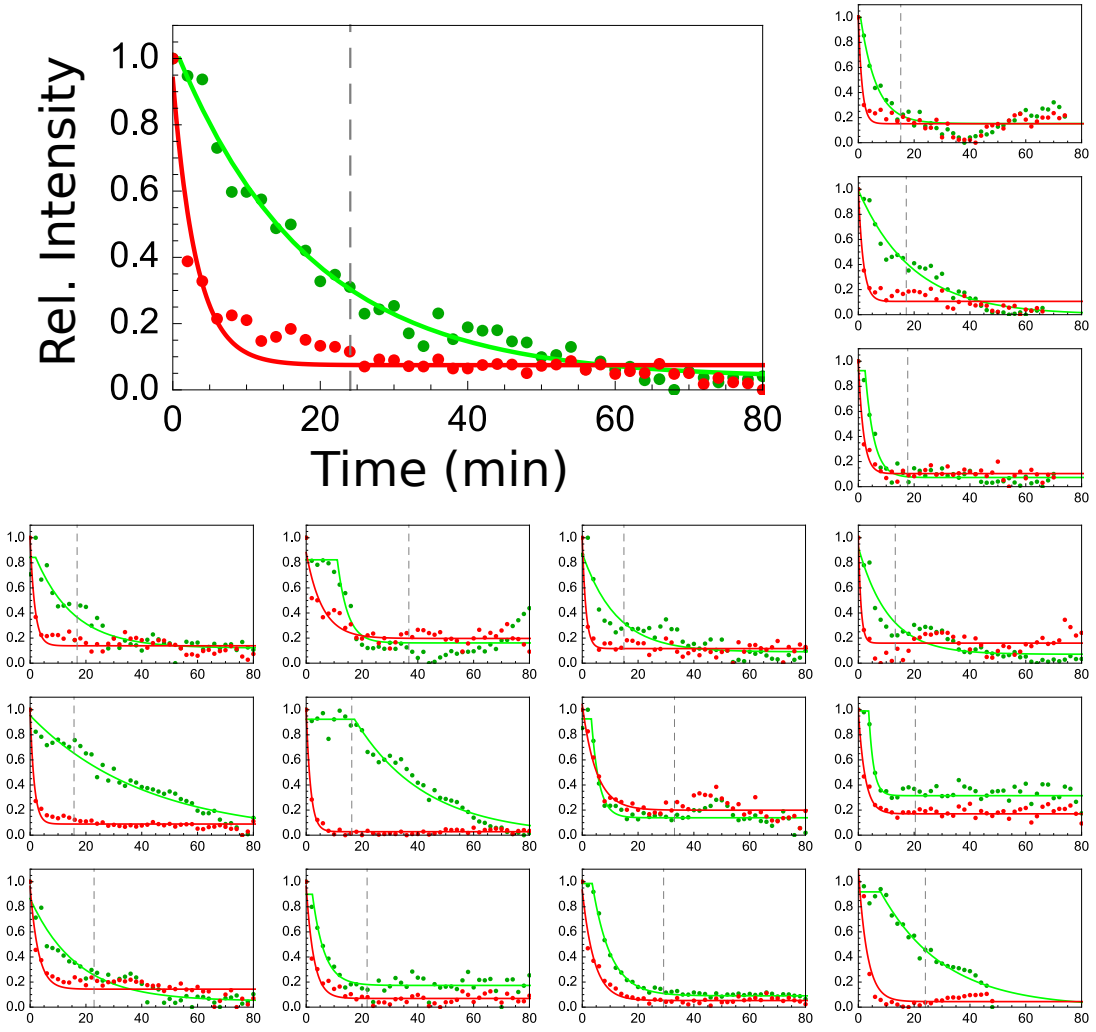

FIGURE 4.6: **Single cell measurements of the decrease in Cherry-tTA-ER transcriptional activator and YFP-MS2 transcripts in U2OS 2-6-3 MeCP2 targeted cells.** The plots show the decrease in YFP-MS2 transcripts (green) and Cherry-tTA-ER transcriptional activator (red) at the reporter gene array in U2OS 2-6-3 cells upon inducing the removal of Cherry-tTA-ER from its tetO binding sequences in the presence of doxycycline and absence of Tamoxifen. The data is fitted to an exponential function with or without a delay for YFP-MS2 and Cherry-tTA-ER dynamics, respectively. The dashed line gives the time point at which Cherry-tTA-ER is depleted from the array with an additionally added 517 seconds of the average RNA polymerase II residence time at the reporter gene. The fitted curves that deviated on average more than 10% from each data point were not used for further analyses.

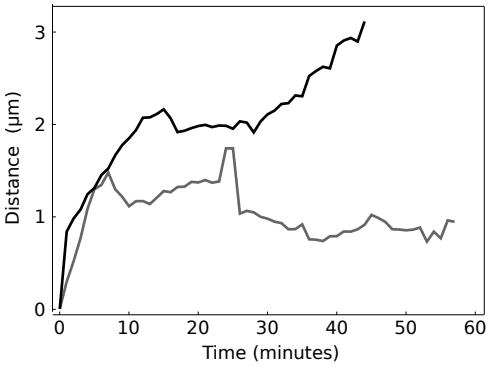

FIGURE 4.7: **Mobility of the transcription spot during transcription repression.** The average displacement of the reporter gene array in U2OS 2-6-3 cells upon inducing the removal of Cherry-tTA-ER from its tetO binding sequence is shown in time for both control (black) and MeCP2 targeted (gray) cells.

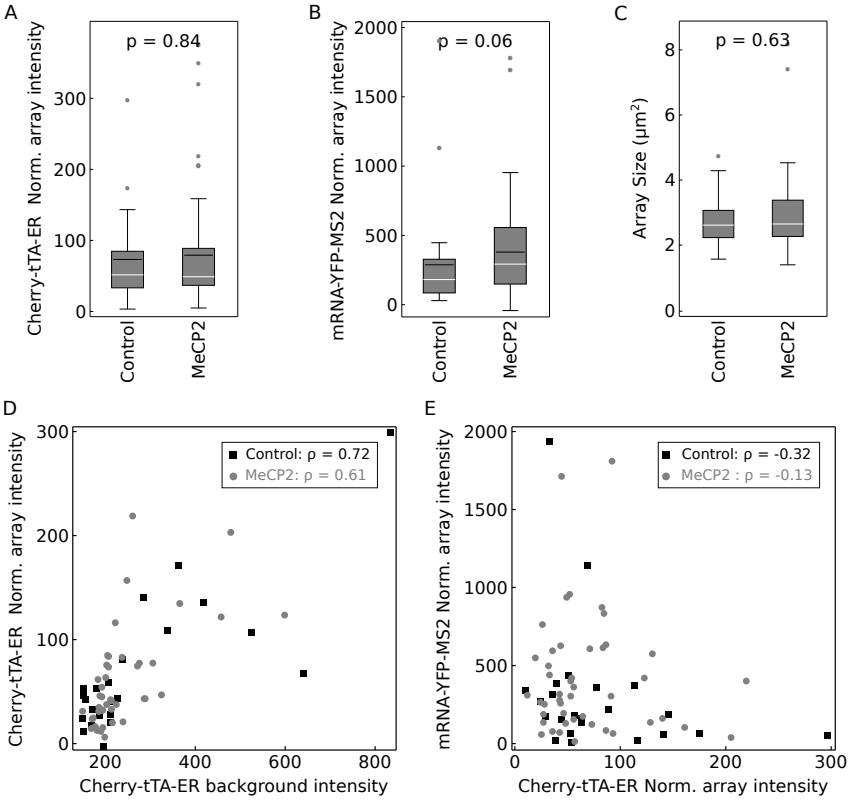

FIGURE 4.8: **Reporter gene array measurements at control and MeCP2 targeted reporter gene array in U2OS 2-6-3 cells.** A) The background-normalized amount of Cherry-tTA-ER transcriptional activator at the reporter gene array in the control and MeCP2 targeted array. B) The background-normalized amount of YFP-MS2 transcripts at the reporter gene array in control and MeCP2 targeted cells. C) The size of the transcription array in control and MeCP2 targeted cells. D) The correlation between transcriptional activator (Cherry-tTA-ER) on the reporter gene array versus random nuclear levels in control cells (circles) and the targeted cells (squares). E) The correlation between transcriptional activator (Cherry-tTA-ER) versus transcript (YFP-MS2) levels at the reporter gene array in control (circles) and MeCP2-targeted cells (squares). In A-C, the p-value shown is obtained with the Mann-Whitney U test In D and E correlation coefficients are given in the inset.

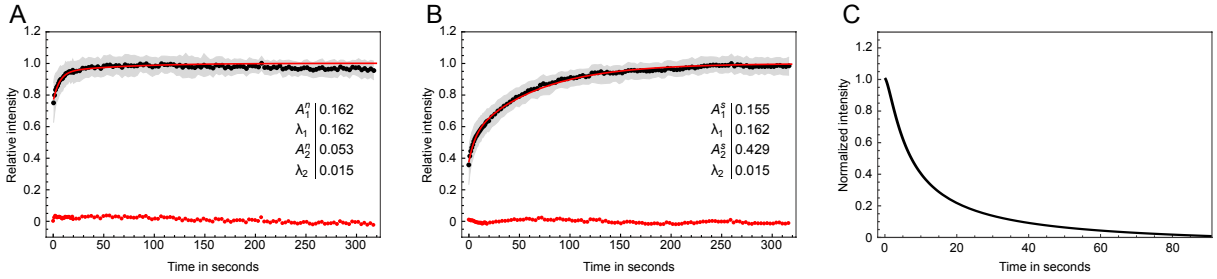

FIGURE 4.9: **YFP-MS2 diffusion kinetics.** (A) FRAP measurements of YFP-MS2 in the nucleus of U2OS 2-6-3 cells. Two different YFP-MS2 fractions can be distinguished representing freely diffusing and bound YFP-MS2. (B) FRAP measurements of YFP-MS2 at the gene array in U2OS 2-6-3 cells. Two different YFP-MS2 fractions can be distinguished representing freely diffusing and bound YFP-MS2. The black dots show the mean of 20 individual FRAP experiments. The gray shaded areas show the standard deviation around this mean. The red line gives the least squares fit to the data points with the residual shown by the red dots. Table 1 summarizes the parameters of the bi-exponential fit, with the fractions of YFP-MS2 (A_1) and mRNA-YFP-MS2 (A_2) of either the nucleus denoted by (n) or the reporter gene array denoted by (s) and the rate constants denoted by $\lambda 1$ and $\lambda 2$. (C) Based on the diffusion parameters, the data are simulated with a diffusion model. The diffusion model simulation shows that upon instant transcription termination the intensity of the transcription spot exhibits a half-life of 7.9 seconds.